Available online at www.sciencedirect.com
SCIENCE DIRECT®
Journal of Nuclear Materials 337–339 (2005) 548–552
journal of nuclear materials
www.elsevier.com/locate/jnucmat

Comparison of deuterium and hydrogen experiments in the Sustained Spheromak Physics Experiment

R.D. Wood *, D.N. Hill, E.B. Hooper, H.S. McLean, D. Ryutov, S. Woodruff

Lawrence Livermore National Laboratory, 7000 East Ave L-637, Livermore CA 94550-9234, United States

Abstract

In this paper we report on the results of deuterium and hydrogen experiments in the Sustained Spheromak Physics Experiment (SSPX). We have compared ~500 deuterium discharges with similar discharges in hydrogen. Typically, we produce H_2 plasmas with peak toroidal currents in the range of 0.6 MA, electron temperatures (T_e) of ~200 eV and energy confinement times (τ_E) of ~200 μs. The D_2 fueled discharges show similar results to those with H_2 fueling with no obvious differences in confinement time. Electron temperatures of ~200 eV with similar electron densities were observed. Both the deuterium and hydrogen fueled discharges have a calculated thermal diffusivity below $\chi_e < 10\ m^2/s$. However, the D_2 fueled discharges had a factor of ~5 increase in high-Z (titanium) impurity content suggesting an increase of physical sputtering. We find no significant mass scaling effects.

Keywords: Deuterium inventory; Impurities; Sputtering

1. Introduction

In this paper we discuss the results of fueling experiments with hydrogen and deuterium on the SSPX (Sustained Spheromak Physics Experiment) spheromak device. The SSPX is a magnetized coaxial gun-driven toroidal confinement device with plasma currents produced by the plasma dynamo rather than by external coils which link the vacuum vessel; this configuration offers the possibility of a less expensive fusion reactor. Analysis of previous spheromak experimental data [1,2] suggested that adequate core energy confinement could be obtained in these devices and that performance might scale favorably to power reactors. The SSPX device was built to explore spheromak confinement and current drive.

The spheromak plasma in SSPX is confined within an $R = 1.0$ m, $h = 0.5$ m, 1.2 cm thick conducting copper shell (flux conserver) which maintains the plasma shape due to image currents flowing in it. A cross section of SSPX is shown in Fig. 1; magnetic flux surfaces for an ideal MHD equilibrium computed with the CORSICA code [3] are included. The thin scrape-off layer region (less than 1 cm wide at the mid-plane) is connected to the electrode near the top of the injector. The gun-injected current of 200 kA produces plasmas with 600 kA of toroidal current and peak magnetic field (B_0) of ~1 T. The typical pulse length is 3.5 ms with peak $T_e > 200$ eV and $n_e = 0.7 - 1.0 \times 10^{20}\ m^{-3}$.

Isotope scaling of transport is an important issue for magnetic fusion. Improvements in plasma performance,

* Corresponding author. Tel.: +1 925 4234691; fax: +1 925 4246401.
E-mail address: wood11@llnl.gov (R.D. Wood).

0022-3115/$ - see front matter © 2004 Elsevier B.V. All rights reserved.
doi:10.1016/j.jnucmat.2004.10.125

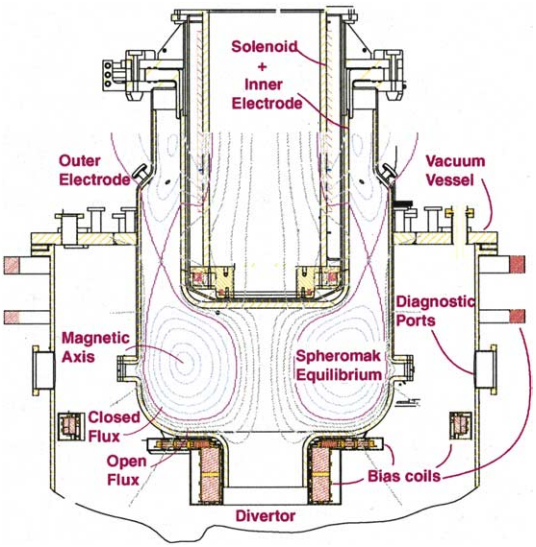

Fig. 1. SSPX with Corsica equilibrium profile.

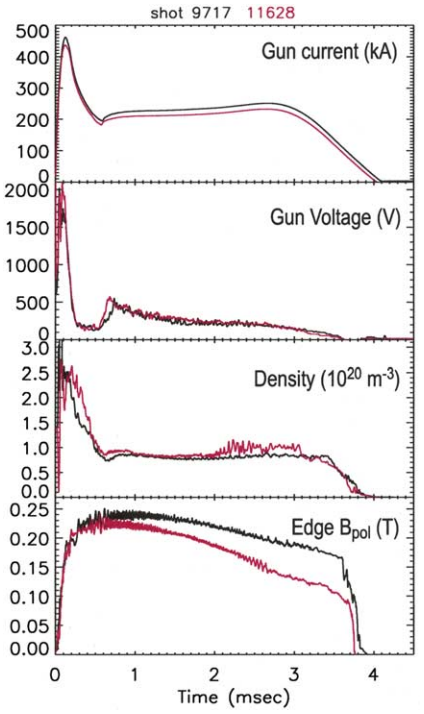

Fig. 2. Time history of SSPX discharge with hydrogen (black) and deuterium (red); gun current, gun voltage, electron density and midplane edge poloidal field.

e.g. energy confinement time (τ_E), have been observed in tokamak discharges with deuterium fueling and a small, but reversed, effect in the ATF stellarator [4]. In tokamaks, the electron temperature is higher in deuterium-fueled discharges than in hydrogen. Many of the improvements in tokamak performance are attributed to changes in both the core and the edge/divertor properties that affect energy and particle transport.

In the remainder of this paper we present improved operation of the SSPX (Section 2), discuss surface conditioning, density control and gas inventory exchange in Section 3, and in Section 4 present results from deuterium fueled operations.

2. Improved spheromak operation

On SSPX the four phases of a discharge include breakdown, formation, sustainment, and decay. A time history of a typical discharge is shown in Fig. 2. Fueling gas is puffed into the injector region ~250 μs before connecting the high voltage formation bank. Breakdown occurs when the gas pressure in the injector region meets, or exceeds, the requirement for Paschen breakdown. Following breakdown, the plasma current (I_{gun}) in the injector region rises sharply for ~100 μs. When the increasing gun current reaches a threshold condition, the $\mathbf{J}\times\mathbf{B}$ force on the plasma in the injector accelerates it out of the injector into the flux conserver region to form the spheromak plasma. The ejection threshold condition occurs when the $\mathbf{J}\times\mathbf{B}$ pressure of the injector toroidal magnetic field becomes greater than the restoring force due to the injector radial bias magnetic flux (Φ_{gun}).

After breakdown and ejection of plasma into the flux conserver, if no additional energy is supplied, the spheromak disconnects from the injector and the current decays on a time scale consistent with resistive dissipation of the magnetic fields; these are formation only discharges. When additional energy is supplied from the sustainment bank via a pulse forming network that supplies constant current for ~3 ms, the plasma can be sustained for a longer period of time. During the sustainment phase, the current from the gun drives reconnection processes that sustain and enhance the poloidal flux. Generally, the radiative losses are low and the decay is very gradual until the bank runs out of energy. As the gun current ramps down at the end of the discharge, the full duration discharges usually terminate abruptly due to MHD activity.

During spheromak formation, the poloidal field builds rapidly and is sustained by driving an instability of the open flux, a toroidal $n = 1$ mode, which in turn provides fluctuations for a MHD dynamo to drive toroidal current. The $n = 1$ mode provides the fluctuation power that couples current from the open flux into the spheromak. Higher order edge magnetic turbulence ($n = 2, 3, 4$) then causes current to distribute throughout the spheromak and as a result the current in the core decays less rapidly than current at the edge. During sustainment excessive edge current and fluctuations

degrade confinement. Optimal operation is obtained by flattening the profile of $\lambda = \mu_0 j/B$, consistent with reducing the drive for tearing and other MHD modes, and matching of edge current and bias flux to minimize $|\delta B/B|_{\rm rms}$. With these optimizations, the highest measured T_e (~250 eV, peaked at the magnetic axis) and lowest core thermal diffusivity ($\chi_e \sim 10$–$20\ m^2/s$) have been obtained.

3. Surface conditioning, density control and gas inventory exchange

To prevent sputtering of the copper conducting shell, the plasma facing surfaces are coated with a 100 μm thick layer of high-pressure plasma-sprayed (HPPS) tungsten. Characterization of the HPPS tungsten surface shows interconnecting layers capable of absorbing high levels of water and fueling gas [5]. Standard wall conditioning techniques are employed to reduce water and carbon levels [6]. Baking to 170 °C for ~100 h reduces the partial pressure of water by an order of magnitude. Hydrogen glow discharge cleaning (GDC) for ~30 h during the bake provides a modest reduction of volatile (CH_4, CO, CO_2) gas species. Helium shot conditioning and titanium gettering further reduce impurities and lead to improved plasma performance.

The performance of spheromaks is sensitive to the plasma density and impurity content since low temperature resistive plasmas have lower confining magnetic fields and corresponding worse confinement than hotter plasmas because currents in the plasma produce the fields. A key measure for the spheromak is the quantity I/N (equivalently j/n), which can be related to the ratio of ohmic heating input power to impurity radiation loss power. When j/n is greater than about 10^{-14} A m, the ohmic heating will exceed the impurity radiation loss and the electron temperature will be transport limited. The evolution of the density after formation depends on whether the current in the spheromak (as opposed to the injector current) is sustained or is decaying. In sustained spheromaks the density depends strongly on whether the sustaining current is above the spheromak formation threshold, expressed as $\lambda = I/\psi$, where I is the current and ψ is initial vacuum magnetic flux threading the injector region. If below threshold, then there is only a weak dependence on λ since most of the current and plasma remain in the injector region. As the current rises above the threshold, the injector plasma is swept out into the main chamber so that the spheromak density can be maintained at a high level.

To ensure the experiments were carried out in deuterium, wall-conditioning techniques were employed in order to exchange the hydrogen-dominated wall with deuterium; a residual gas analyzer was used to monitor the partial pressures of deuterium and hydrogen gases. Four hours of GDC in D_2 was followed by ~100, short duration, formation only conditioning discharges. The conditioning discharges use only the stored energy in the formation bank (500 kJ) so that more discharges can be obtained more rapidly using less energy. The working gas for the conditioning discharges was alternated between helium and D_2. Helium shot conditioning reduces the production of volatile impurity species pressures by reducing the carbon and oxide layer on the metal surface. In addition to GDC and conditioning discharges, ~50 full duration discharges with deuterium fueling were required to increase the measured D_2 partial pressure by 50× and reduce the atomic hydrogen gas level by about an order of magnitude.

4. Deuterium plasmas

During deuterium operations, the combined gas-puff-to-breakdown time increased from 550 μs (hydrogen fueled) to 790 μs. The increased delay time is consistent with isotopic mass scaling of the sound speed. A time history comparing two discharges, one fueled with hydrogen and the other deuterium, is shown in Fig. 2. With the exception of the deuterium gas puff timing, the programmed shot parameters (gun flux, bank voltages and fueling pressure) for both discharges are identical. The gun current for the deuterium discharge is ~10% less than the gun current for the hydrogen discharge while both discharges have similar gun voltage and electron density time traces. Since the resistance of the external electrical circuit is constant, the change in gun current and constant gun voltage correlates with an increase in plasma resistivity for the deuterium discharge. Furthermore, the measured edge poloidal magnetic field for the deuterium discharge is less and is decaying more rapidly, consistent with an increase in plasma resistivity. In subsequent deuterium discharges, to achieve the same injector current and voltage as the hydrogen fueled discharge (shot 9717), more bank energy was required. The increased plasma resistivity and more rapid magnetic field decay time correlates with an increase in impurity radiation for the deuterium discharges.

To characterize the impurity radiation, line emissions in the 100–1600 Å spectral region are measured using an absolutely calibrated SPRED spectrograph [7]. The spectrograph has a tangential view of the magnetic axis through the midplane and provides a time-integrated spectrum of the discharge. As seen in Fig. 3, the measured spectrum for the deuterium discharge shows an increase in titanium line emissions while the oxygen line emissions are similar. The titanium emissions typically increased by a factor of ~5 and are attributed to an increase in the sputtering yield of titanium by deuterium ions. At spheromak relevant ion temperatures

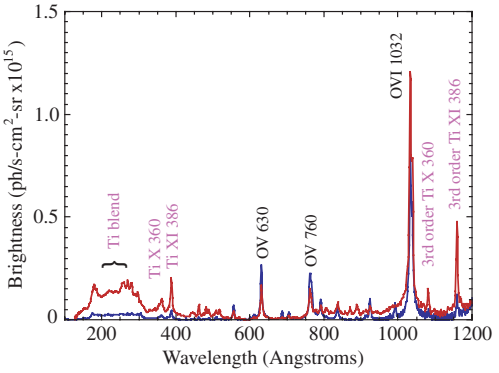

Fig. 3. Time-integrated spectrum of hydrogen (blue) and deuterium (red) discharge showing increased titanium emissions.

($T_i = T_e \sim 150$ eV during sustainment) and sheath voltages (~300 V), the sputtering yield of titanium by deuterium is an order of magnitude greater than sputtering by hydrogen ions [8]. Because measured impurity concentrations are not available, an energy balance analysis is used to determine the effect of the increased titanium emissions on plasma performance. Spectroscopic analysis of measured impurity emissions for an ensemble of H_2 and D_2 fueled discharges show a 40% increase in the total radiated energy (J/cm^2) due mostly to an increase in titanium line emissions for the D_2 discharges. Table 1 lists the energy input (E_{input}) to build to the maximum field, the magnetic field energy ($W_B@t = 3$ms), and the radiated energy (E_{rad}) from spectroscopy for D_2 and H_2 discharges with the same E_{input} and a D_2 discharge with increased E_{input}. The D_2 discharge with the same $E_{input} = 115$ kJ as the H_2 discharge has less magnetic field energy and more impurity radiated energy. In an attempt to obtain a discharge in D_2 with the same magnetic field energy as the H_2 in Table 1, the input energy was raised from 115 kJ to 133 kJ. More energy went into the magnetic field, however the E_{rad} also increased due to increased titanium emissions. The decrease in stored magnetic energy for the deuterium-fueled discharges is attributed to an increase in radiation due to increased titanium emissions.

Table 1
Energy balance comparison of D_2 and H_2 fueled discharges

	H2 (9717)	D2 (11628)	D2 (12372)
E_{input} (formation)	115	115	133
W_B (mag. field)	14	9	12
E_{rad} (impurities)	63	77	98

E_{rad} is determined from spectroscopy assuming the measured emissions are uniformly distributed over the plasma volume. All values are in kJ.

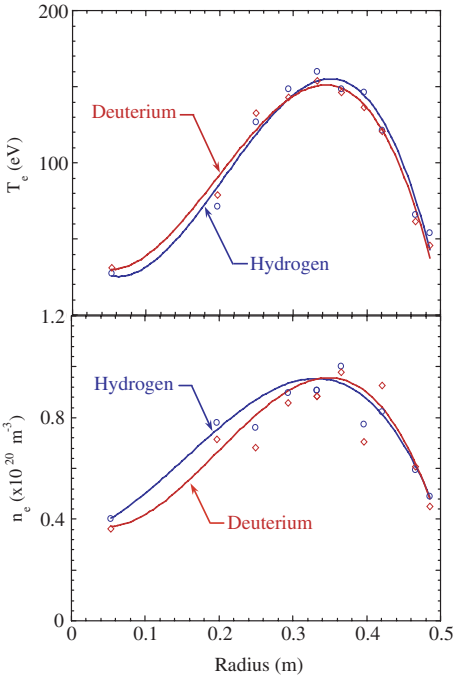

Fig. 4. Electron temperature and density profiles comparing hydrogen (circles) and deuterium (diamonds) discharges; measurement time is ~2.0 ms after breakdown.

Measured radial profiles of T_e and n_e, for both deuterium and hydrogen fueled discharges are essentially identical in shape and magnitude. Approximately 100 discharges with similar operating parameters were obtained with a peak T_e greater than 100 eV. Those discharges have been averaged to eliminate shot-to-shot variations in the T_e and n_e profiles shown in Fig. 4. The radial profiles are peaked at the magnetic axis and are parabolic in shape. Because confinement time is dominated by the edge power associated with the fields we focus on χ_e, instead of τ_e. The experimentally

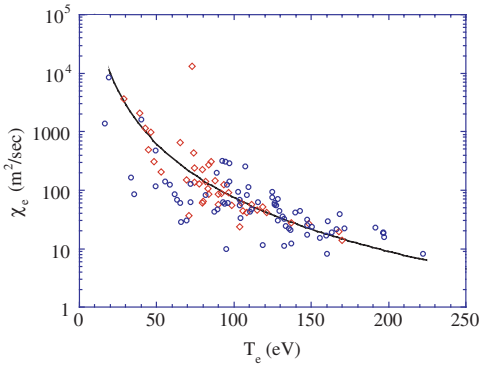

Fig. 5. CORSICA calculated thermal diffusivity, χ_e, for hydrogen (circles) and deuterium fueled discharges (diamonds).

determined [9] thermal diffusivity, χ_e, is also independent of fueling gas. Fig. 5 shows a plot of the calculated core χ_e versus peak T_e. At higher T_e, the magnitude of χ_e is Bohm-like but scaling is different for both H_2 and D_2 fueled discharges.

5. Summary

On SSPX, progress has been made in understanding both magnetic field generation and confinement, enabling the production of high ($\sim$1 T) magnetic field spheromaks with core electron temperatures (T_e) of > 200 eV and thermal diffusivity of $\chi_e \sim 10$–20 m^2/s in the plasma core. To build upon these results, experiments with D_2 fueling were conducted to explore possible further improvement in plasma performance as seen in tokamaks. To obtain the same measured plasma parameters, more input energy was required for the D_2 fueled discharges. Furthermore, the measured edge poloidal magnetic field for deuterium discharges was less and decays more rapidly. The increased input energy and a more rapid magnetic field decay time correlates with an increase in plasma resistivity. Spectroscopic measurements showed a factor of $\sim$5 increase in titanium line emissions. The increased titanium emissions are attributed to an increase in the sputtering yield of titanium by deuterium ions. With higher input energy, the D_2 fueled discharges show similar results to those with H_2 fueling. Electron temperatures of $\sim$200 eV with similar electron densities were observed. Isotope mass effects are not observed on SSPX.

Acknowledgments

This work was carried out under the auspices of US DOE by the University of California Lawrence Livermore National Laboratory under Contract W-7405-ENG-48.

References

[1] T.K. Fowler, J.S. Hardwick, T.R. Jarboe, Comments Plasma Phys. Control. Fus. 16 (1994).
[2] E.B. Hooper, J.H. Hammer, C.W. Barnes, et al., Fus. Technol. 29 (1996).
[3] E.B. Hooper, L.D. Pearlstein, R.H. Bulmer, Nucl. Fus. 39 (1999) 863.
[4] M. Bessenrodt-Weberpals et al., Nucl. Fus. 33 (1993) 1205.
[5] D.A. Buchenauer, B.E. Mills, R.D. Wood, et al., J. Nucl. Mater. 290–293 (2001) 1165.
[6] R.D. Wood et al., J. Nucl. Mater. 290–293 (2001) 513.
[7] R.J. Fonk, A.T. Ramsey, R.V. Yelle, Appl. Optics 21 (1982) 2115.
[8] E.W. Thomas, Atomic Data for Control. Fus. Res. 3 (1985) A10.
[9] H.S. McLean et al., in: Proceedings of the 30th European Conference on Control. Fus. and Plasma Phys., vol. 27A, 2003, P-3.230.